Dynamics of Electron Localization, Solvation, and Migration in Polar Molecular Clusters

R. N. Barnett,[1] Uzi Landman,[1] and A. Nitzan[2]
[1]*School of Physics, Georgia Institute of Technology, Atlanta, Georgia 30332*
[2]*School of Chemistry, Tel Aviv University, 69978, Tel Aviv, Israel*
(Received 19 August 1988)

The time evolution of electron localization, migration, and solvation in water and ammonia clusters is investigated via computer simulations. The attachment of an electron to a cold molecular cluster in a diffuse weakly bound surface state, the dynamics of solvation, the nonhopping mechanism of migration leading to the formation of an internally solvated state, and the spectral manifestation of these processes are demonstrated.

PACS numbers: 71.55.Jv, 31.70.Dk, 36.40.+d, 61.20.Ja

Advances in ultrafast time-resolved spectroscopy[1,2] and recent theoretical developments[3] open new avenues for investigation on refined temporal and spatial scales of the dynamics and mechanism of electron solvation in fluids and in clusters, electron transfer reactions, electrochemical processes, and chemical reactions in solution and of carrier mobility in condensed phases with varying degrees and modes of aggregation.

In this paper we focus on the *dynamics* of electron localization, migration, and solvation in polar molecular clusters. Our studies demonstrate that a cold neutral cluster can attach a low-energy electron[4] in a diffuse weakly bound surface state which evolves into an internally solvated state on a time scale of a few ps. Furthermore, we provide evidence for a nonhopping mechanism of excess-electron migration in polar molecular materials.

Negatively charged free water[4,5] $(H_2O)_n^-$ (for $n \geq 11$) and ammonia[6] $(NH_3)_m^-$ (for $m \geq 30$) clusters have been recently prepared either by localization during the cluster nucleation process[5,6] or via capture of very-low-energy electrons by cold water clusters.[4] Recent theoretical investigations[7,8] employing the quantum path-integral molecular dynamics (QUPID) method revealed that electron localization in polar molecular clusters occurs via surface or internal modes depending on cluster size and chemical composition, yielding results in agreement with experimental observations.

Investigations of the time evolution of the coupled electron-molecular cluster system require methods which allow simulations of the quantum mechanical evolution in conjunction with classical dynamics of the atomic constituents coupled to the excess electron.[3,9,10] Although simulations (within the time-dependent self-consistent-field method[3,9,10]) in which the real-time propagation of the electron is obtained, via a numerical solution of the time-dependent Schrodinger equation, are possible,[9-11] in most of our studies an adiabatic simulation method is used[10] where the electron is constrained to remain in a given state (in this paper the ground state) and is described by a wave function which corresponds to the instantaneous (dynamical) nuclear configuration. The method, when used within the validity of the Born-Oppenheimer approximation, allows efficient investigations of the detailed dynamical mechanisms and spectroscopy[10,12] of electron localization, penetration, and solvation.[3,10]

The operation by which the electron is constrained to the ground state is achieved via the split-operator fast-Fourier-transform method,[9] while the classical (atomic) degrees of freedom evolve, of course, in real time. In the application of this method, which is performed on a three-dimensional grid, caution was exercised to assure adequate grid spatial extent and grid spacings [initially ($t \leq 0.168$ ps), grids of $N_g = 32^3$ points and grid spacing $\Delta = 2a_0$ were used; subsequently, $N_g = 16^3$ and $1.5a_0 \leq \Delta \leq 2.0a_0$], and a "moving grid" technique was developed to assure that the wave function is faithfully represented on the grid throughout.[13]

The interactions between the electron and ground-state cluster molecules were described via a pseudopotential developed and used by us previously[7,8] in extensive QUPID studies of electron solvation in water and ammonia clusters that yielded results in quantitative agreement with experimental data. For the intermolecular interactions in ammonia we have employed the potential proposed by Hinchliffe *et al.*[14] (model C), augmented by intramolecular interactions using a harmonic valence-coordinate model potential.[8] The RWK2-M potential was used for water.[15]

We start our simulations from a system in which a ground-state excess electron is initially attached to an equilibrated neutral 256-molecule cluster at 189 K for ammonia and 300 K for water. In the initial state (for ammonia see Fig. 1), the electron is weakly bound ($E_0 = -0.011$ hartree for ammonia and -0.008 hartree for water) to the molecular cluster in a diffuse surface state, consistent with the lack of preexisting deep traps in bulk polar liquids.[2,3,16] The time variations of energetic and structural characteristics during the subsequent dynamical evolution, shown in Figs. 2 and 3, exhibit four temporal stages.

(1) $t \leq 0.15$ ps for both systems.—The initial time evolution is characterized by a reorientation of the cluster environment coupled to an increase in the magnitude of the ground-state energy of the excess electron

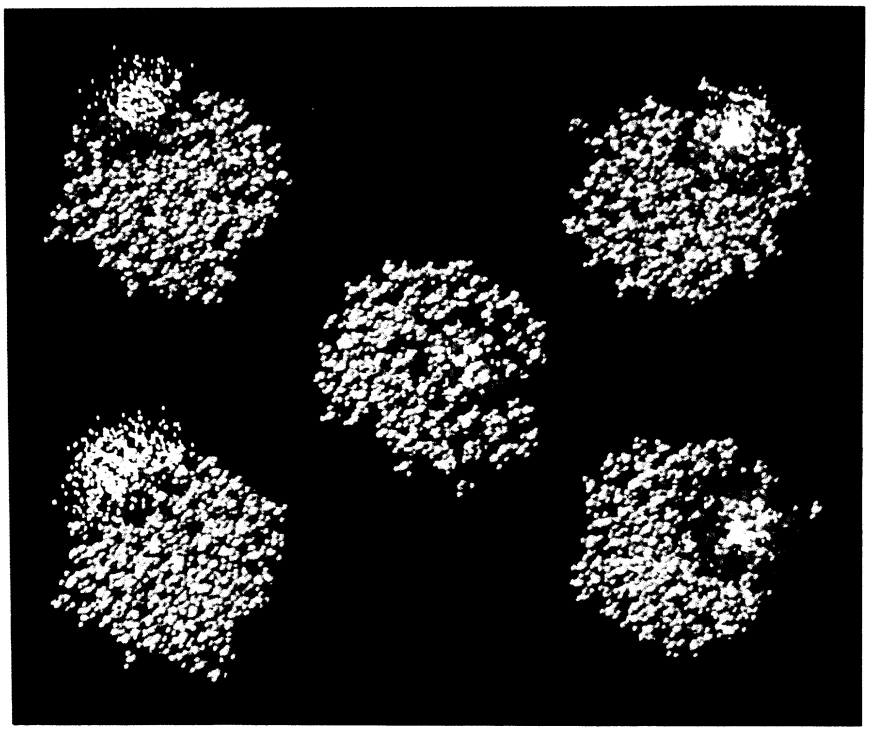

FIG. 1. Snapshots of cluster configurations and the electron distribution (white dots) at various stages of the dynamical evolution for $(NH_2)_{256}^-$. From bottom left and clockwise: $t=0$, 0.16, 3.0, 4.85, and 18.48 ps (center). Color code: red, green, blue, and yellow correspond to molecules in shells $(0,7.5a_0)$, $(7.5a_0,10a_0)$, $(10a_0,15a_0)$, and $(>15a_0)$, respectively, about the center of the electron density distributions.

(-0.045 and -0.03 hartree for ammonia and water, respectively, at $t=0.15$ ps), an increase in the separation between the ground and first excited states, and a transition to a compact wave function [see Fig. 1, and the initial drop in the width of the wave function, $r_g=\langle\psi_0|\times r^2|\psi_0\rangle^{1/2}$, in Fig. 2(b)]. While at the very beginning of this initial stage the assumptions underlying the ground-state-dynamics method are not fully satisfied, subsequent time evolution is described faithfully by this method (as substantiated by comparing the ground-state-dynamics results with those obtained via real-time propagation of the electronic wave function, within time-dependent self-consistent-field approximation, without the ground-state constraint).

(2) $0.15\leq t\leq 3$ ps ($0.15\leq t\leq 1.2$ ps for water). —During this stage the excess electron remains bound in a surface state [see the distance, $r_{e\text{-c.m.}}$ between the center of density of the electron, $\mathbf{r}_e$, and the cluster center of mass, in Fig. 2(b)], exploring various sites on the surfaces of the cluster. Accompanying the motion of the electron is an increase in the magnitude of E_0 [Fig. 2(a)], a gradual variation in the excitation spectrum [shown for water in Fig. 2(c)], and a significant reorganization of the molecular cluster, mainly in the vicinity of the electron, evidenced by increases in the intermolecular potential energy and in the magnitude of the cluster dipole moment, and by the high degree of molecular orientation with respect to the electron [see Fig. 3(b), where the time variation of the molecular dipole orientations in three molecular shells around $\mathbf{r}_e$ is shown for ammonia]. While during this stage the electron is confined mainly to the outer region of the cluster, the initial stage of the electron solvation process begins as evidenced by an increase in the number of near-neighbor molecules (particularly in the distance range $7.5a_0$–$10a_0$) seen in Fig. 3(a), where the number of neighbors decomposed into molecular shells is shown. Similar results were obtained for water. The ammonia cluster configuration and the electron density at $t=3$ ps are shown in Fig. 1.

(3) $3<t\leq 5$ ps ($1.2\leq t<1.5$ ps for water). —Following the formation of a well-bound surface state during stage 2, the systems evolve in a dramatic manner signified by sharp changes in energetic and structural characteristic quantities. In this stage the first molecular solvation shell around the excess electron is completed in both systems. As seen in the inset of Fig. 3(a) the number of ammonia molecules within $7.5a_0$ from $\mathbf{r}_e$ (subshell s1a) increases suddenly to about 6 (at ~ 3.3 ps), and fluctuates about this value for the remainder of the simulation. In conjunction with the formation of the solvation cavity the excess electron density contracts [see r_g in Fig. 2(b)] and the center of density penetrates toward

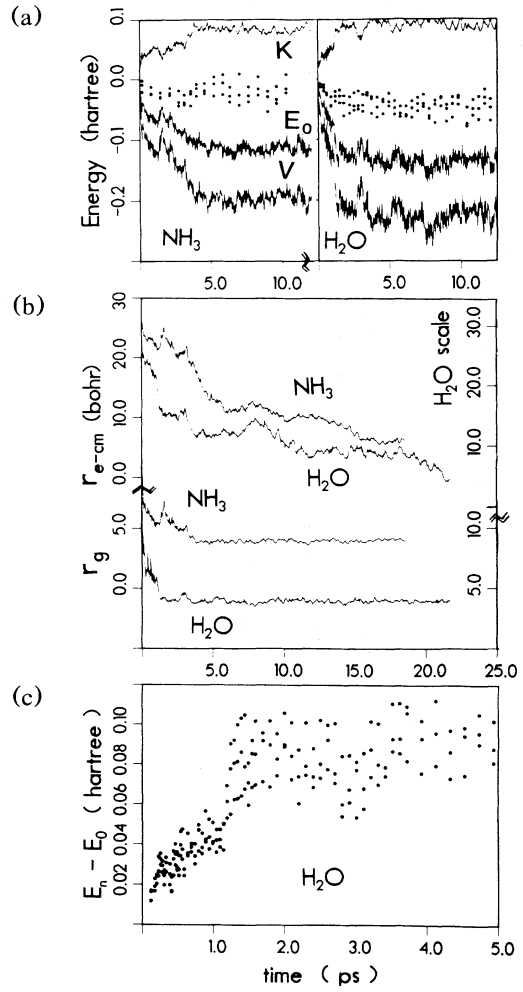

FIG. 2. Time evolution of the excess electron in the ammonia and water clusters. (a) The electron ground-state energy E_0 and the potential (V) and kinetic (K) energy contributions, for $0 \leq t \leq 12.5$ ps. The first three excited states are given at selected times by the dots. (b) Width of the electron distribution, r_g, and distance from the cluster center of mass, $r_{e\text{-c.m.}}$. NH_3 and H_2O scales on left and right, respectively. (c) The excitation spectrum, $E_n - E_0$, $n = 1$–3, for $(H_2O)_{256}^-$, for $0 \leq t \leq 5$ ps. No significant variations in energetic properties occur beyond the time spans shown.

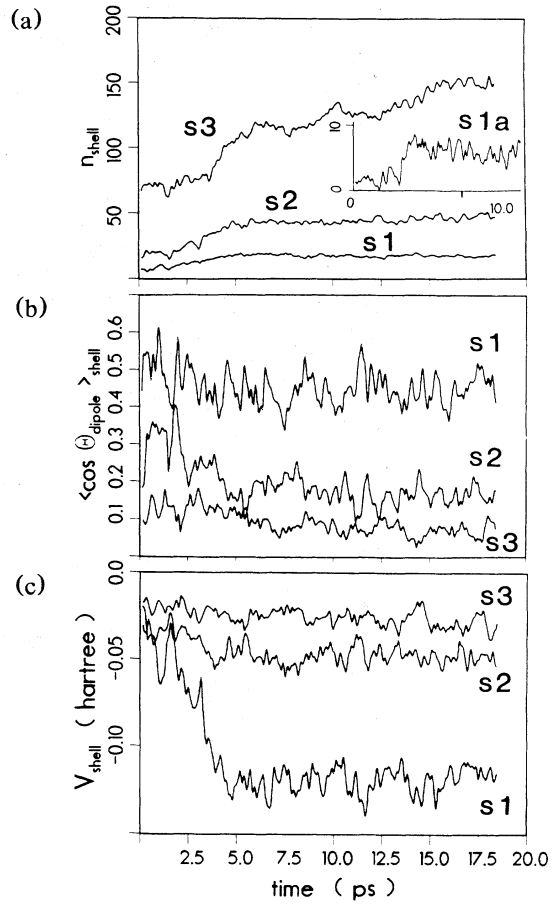

FIG. 3. (a) The number of ammonia molecules n vs time in shells around the center of the electron density, $\mathbf{r}_e$: s1 $(0,10a_0)$; s2 $(10a_0,15a_0)$, and s3 $(15a_0,25a_0)$. Inset: n in the subshell s1a $(0,7.5a_0)$. The choice of shells is guided by the molecular distribution about the fully solvated electron (Ref. 8). (b) Time variation of the cosine of the angle between $\mathbf{r}_e$ and the ammonia molecular dipoles in shells. (c) Time variation of the electron–ammonia-cluster interaction potential decomposed into molecular shells.

the center of the cluster. Additionally the formation of the first solvation shell results in a decrease in the orientational order of more distant molecules [Fig. 3(b)] and a decrease in the total cluster dipole moment due to screening of the excess electron charge by the first solvation shell. A snapshot of the molecular configuration and electron density distribution at the end of this stage is shown in Fig. 1. The $(H_2O)_{256}^-$ system exhibits a similar behavior during this stage (which is of shorter duration).

These structural changes are accompanied by pronounced sudden changes in the excess-electron ground-state potential and kinetic energies [Figs. 2(a)] and excitation energies [see spectrum for the water cluster in Fig. 2(c)]. Note that these changes occur in less than 1 ps in both systems and correlate with the sudden increase in the number of molecules within $7.5a_0$ of $\mathbf{r}_e$. The values of the electron ground-state energy E_0 and excitation energies at the end of this fast stage are close to those of the fully solvated electron. In this context we note that the calculated sudden increase in the excitation energies, which would exhibit itself as a shift of the absorption spectrum to shorter wavelength, is reminiscent of the shift in the absorption spectrum from an initial absorption peaking in the infrared to an absorption maximum at the wavelength characteristic of the fully solvated electron observed in recent studies of the dynamics of excess-electron solvation in liquid water following photo-

ionization,[2] and in theoretical studies of electron solvation.[3]

(4) $t > 5$ ps ($t > 1.5$ ps for water).—Having established in stage 3 a local environment characteristic of a fully solvated electron, the systems continue to evolve with the electron migration towards the center of the cluster accompanied by gradual buildup of successive solvation shells [see Fig. 3(a) for the ammonia cluster]. A snapshot of a cluster configuration and the excess electron density at the end of the simulation is shown in Fig. 1 (center).

The molecular reorganization of the cluster coupled to the quantum-mechanical evolution is essential for the formation of the solvated state, which does not develop if the cluster (classical) degrees of freedom are frozen in their initial-state configuration. Studies of *F*-center-like excess-electron migration in molten salts[11] suggest that the electron transport in these systems is mostly due to short-time jumps between two spatially separated sites, characterized by the occurrence of configurations where at the intermediate time (between sites) the wave function exhibits splitting and a potential barrier separates the initial and final localized states of the electron.[11] In our simulations we did not find evidence for such hopping events; i.e., configurations characterized by a bimodal distribution of the electron density were not found. Such events would have been exhibited in large variations in the width of the electron distribution, r_g, which are absent in our simulations [see Fig. 2(b)].

The difference between the electron migration mechanisms may be attributed to the difference in the host reorganization energy in these systems. In the case of molten alkali halides the solvated electron substitutes for a halide anion and the energy of the region containing the electron is close to that of neighboring regions in the fluid. On the other hand, in a polar molecular system the energy of a region around the solvated excess electron is much larger in magnitude than that of an equivalent neighboring neutral region. Furthermore, in the latter case, because of the sizeable reorganization energy[7,8] which accompanies the formation of the solvation shells, solvent fluctuations leading to a favorable solvation site in a neutral region are unlikely. Indeed, the absence of deep traps in neutral water has been recently demonstrated.[16]

As shown by our previous QUPID calculations[7,8] the adiabatic binding energy (i.e., the electron ground-state energy plus the cluster reorganization energy) of an excess electron to a polar molecular cluster favors internal localization for sufficiently large clusters [$n \gtrsim 64$ for $(H_2O)_n^-$ and $n \gtrsim 32$ for $(NH_3)_n^-$]. In addition, a continuum dielectric model for excess electrons in finite molecular aggregates[7,17] yielded results in agreement with these calculations and experimental data, and demonstrated the importance of the long-range polarization interaction in stabilizing the solvated state. As seen from Figs. 3(a) and 3(c) (with similar results for water), while the largest contribution to the electron potential energy comes from its interaction with the first solvation subshell (0–$7.5a_0$), which is fully developed at an early stage [see Fig. 3(a)], the long-range interaction with the molecular shells furthest away [Fig. 3(c)] and the development of these shells [Fig. 3(a)] provide the driving force for migration from the surface to the interior. The mechanism of migration is polaronlike in nature, with the electron propagating in a spatially localized solvated ground state via polarization of the dynamical host environment (no "dragging" of molecules accompanies the migration of the electron). The spectral consequences [i.e., the sudden increase in the excitation energy, see Fig. 2(c)] of the time evolution of the electron-cluster system remain an experimental challenge.

This research was supported by U.S. DOE Grant No. FG-05-86ER45234.

[1]See review by J. D. Simon, Acc. Chem. Res. **21**, 128 (1988); M. Marconcelli, E. W. Castner, Jr., S. P. Webb, and G. R. Fleming, in *Ultra-Fast Phenomena V,* edited by G. R. Fleming and A. E. Siegman (Springer-Verlag, Berlin, 1986), p. 303, and references therein.

[2]A. Migus, Y. Gauduel, J. L. Martin, and A. Antonetti, Phys. Rev. Lett. **58**, 1559 (1987), and references therein.

[3]See review by P. J. Rossky and J. Schnitker, J. Phys. Chem. **92**, 4277 (1988).

[4]M. Knapp, O. Echt, D. Kreisle, and E. Recknagel, J. Chem. Phys. **85**, 636 (1986), and **91**, 2601 (1987).

[5]M. Armbuster, H. Haberland, and H. G. Schindler, Phys. Rev. Lett. **47**, 323 (1981); H. Haberland, H. G. Schindler, and D. R. Worsnop, J. Chem. Phys. **81**, 3742 (1984); J. V. Coe, D. R. Worsnop, and K. H. Bowen, J. Chem. Phys. (to be published).

[6]H. Haberland, H. Langosch, H. G. Schindler, and D. R. Worsnop, Ber. Bunsen-ges. Phys. Chem. **88**, 270 (1984).

[7]R. N. Barnett, U. Landman, C. L. Cleveland, and J. Jortner, Phys. Rev. Lett. **59**, 811 (1987), and J. Chem. Phys. **88**, 4421 (1988).

[8]R. N. Barnett, U. Landman, C. L. Cleveland, N. R. Kestner, and J. Jortner, J. Chem. Phys. **88**, 6670 (1988), and Chem. Phys. Lett. (to be published).

[9]See review by R. Kosloff, J. Phys. Chem. **92**, 2087 (1988); also Ref. 3.

[10]R. N. Barnett, U. Landman, and A. Nitzan, J. Chem. Phys. **89**, 2242 (1988), and Phys. Rev. A **38**, 2178 (1988).

[11]A. Selloni, P. Carenvali, R. Car, and M. Parrinello, Phys. Rev. Lett. **59**, 823 (1987).

[12]J. Schnitker, K. Motakabbir, P. J. Rossky, and R. Friesner, Phys. Rev. Lett. **60**, 456 (1988).

[13]R. N. Barnett, U. Landman, and A. Nitzan, J. Chem. Phys. (to be published).

[14]A. Hinchliffe, D. G. Bounds, M. L. Klein, I. R. McDonald, and R. Righini, J. Chem. Phys. **74**, 1211 (1981).

[15]J. R. Reimers and R. O. Watts, Chem. Phys. **85**, 83 (1984), and **64**, 95 (1982).

[16]K. A. Motakabbir and P. J. Rossky, Chem. Phys. (to be published).

[17]R. N. Barnett, U. Landman, C. L. Cleveland, and J. Jortner, Chem. Phys. Lett. **145**, 382 (1988).

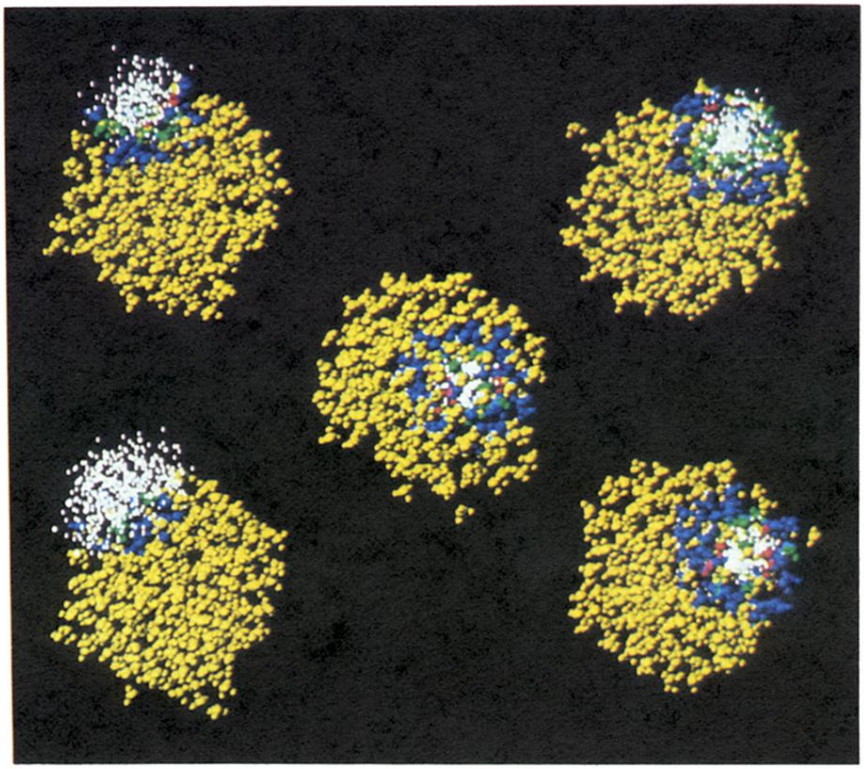

FIG. 1. Snapshots of cluster configurations and the electron distribution (white dots) at various stages of the dynamical evolution for $(NH_2)_{256}^-$. From bottom left and clockwise: $t=0$, 0.16, 3.0, 4.85, and 18.48 ps (center). Color code: red, green, blue, and yellow correspond to molecules in shells $(0,7.5a_0)$, $(7.5a_0,10a_0)$, $(10a_0,15a_0)$, and $(>15a_0)$, respectively, about the center of the electron density distributions.